29th Congress of the International Council of the Aeronautical Sciences
St. Petersburg, Russia; September 7-12, 2014

DYNAMIC LOADS ACTING ON ENGINE FRAME ELEMENTS AFTER FAN BLADE OUT EVENT STUDY

I.I. Ivanov*, B.S. Blinnik*
***Central Institute of Aviation Motors**

Keywords: *fan blade out event, dynamic loads, load reduction device, dynamic turbofan engine model.*

Abstract

Loads acting on gas turbine jet force elements significantly increase after fan blade out (FBO) event due to appearing unbalance. A load reduction device (LRD) is introduced to fan shaft supports for the purpose of unallowable effects avoidance. LRD breaks down under specified loads. LRD actuation causes rotor self-centering and loads acting on engine frame reducing. The special dynamic model is required for calculating engine frame loads after FBO event. During the research work such model of turbofan was developed taking into consideration accounts of stiffness and inertial properties of engine rotors and casings, engine rotors velocities decreasing after fuel turning off and contact interactions between rotors and stators. The effect of LRD introduction in turbofan design and the influence of other design parameters on engine dynamic loads are analyzed.

1 Introduction

Fan blades are subjected to different damages caused by operational loads (static, dynamic) and hits of foreign bodies in the turbine flow. These factors can result onto fan blade full or partial breakage. Loads acting on gas turbine jet engine force elements (bearing supports, frames, mounts, see fig 1) significantly increase in comparison with regular ones after FBO event due to the appearing unbalance. The unbalanced centrifugal force caused by fan blade breakage is typically about 1,000,000 N at the maximum operational LP rotor speed. Standards of airworthiness demand FBO event not to be leading to the catastrophic consequences (engine mounts rupture, case fragments hit into combustion chamber, beginning of a fire, bearings jam).

A load reduction device (LRD, see fig 2) is introduced to fan supports of turbofan's last models to avoid mentioned unallowable effects. This device breaks down under specified loads resulting in the change of engine strength frame and decreasing for supports' stiffness. Fan rotor critical velocity usually becomes lower than its operating rotating frequency and rotor passes from subcritical to supercritical range after LRD actuation, causing rotor self-centering and loads acting on engine frame reducing and redistribution.

The model imitating dynamic altering of forces and displacements in typical turbofan engine design after FBO event is described in the research work. The model takes into account stiffness and inertial properties of engine rotors, casings and mounts, asymmetry of engine fixation relative its axis, engine rotors deceleration after fuel turning off, contact interactions of rotor and stator in LPC by means of blades and also a clearance overlapping between LP and HP rotors. The nonlinear transient problem is solved in the industrial analysis computer program NASTRAN.

2 Model description

Existing methods for analysis of gas turbine jet dynamic behavior after FBO event are based on full 3D finite element (FE) simulation [1, 2]. When using these methods any change in engine design results in the considerable rebuilding of FE model. Therefore full 3D FE modeling is quite inconvenient for analysis of different

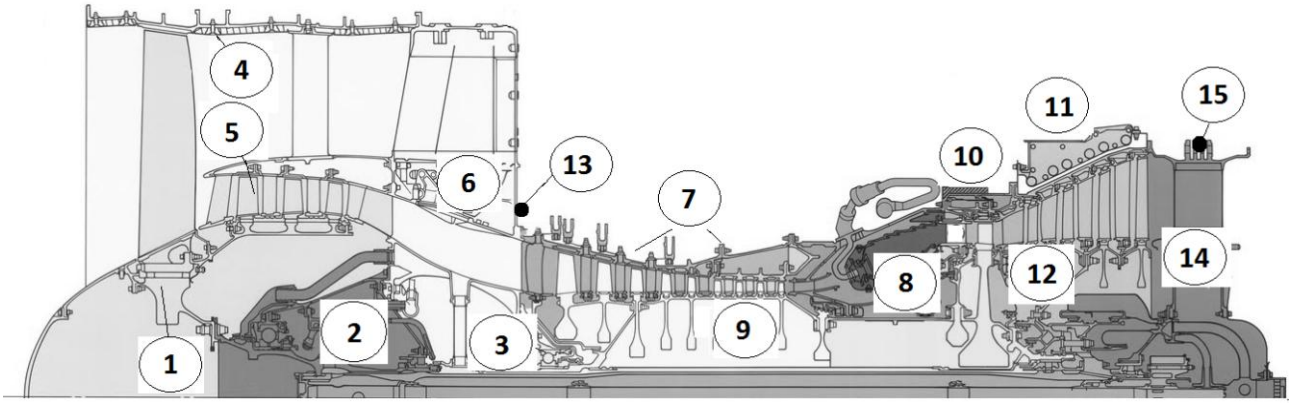

Figure 1. Example of turbofan engine strength circuit.
1 – fan, 2 – fan supports, 3 – inlet gearbox and high pressure compressor (HPC) support, 4 – fan casing, 5 – booster, 6 – intermediate casing, 7 –HPC stator, 8 – combustor casing, 9 – high pressure (HP) rotor, 10 – high pressure turbine (HPT) stator, 11 – low pressure turbine (LPT) stator, 12 – LPT rotor, 13 – forward mount, 14 – LPT support, 15 – rear mount.

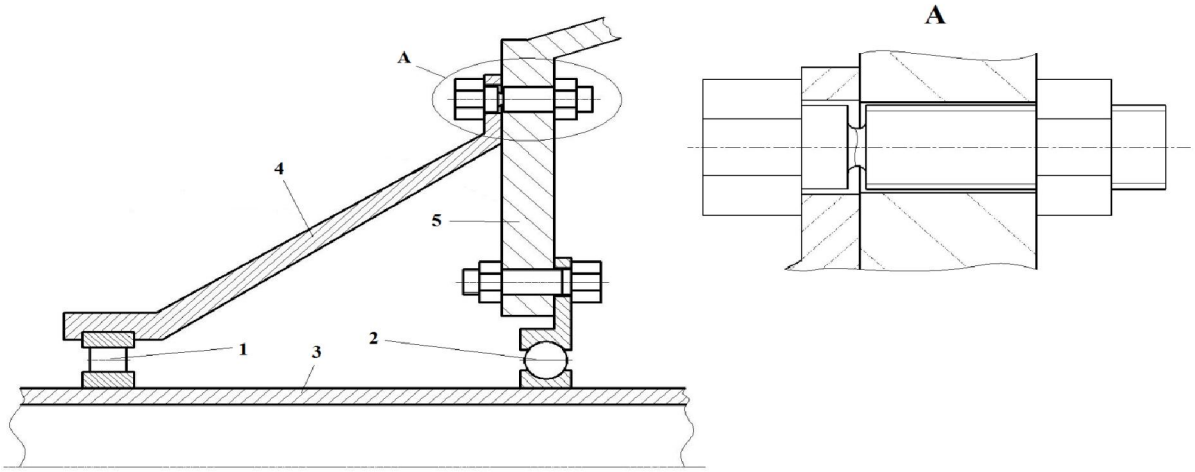

Figure 2. Example of the load reduction device.
1 – bearing №1, 2 – bearing №2, 3 – fan shaft, 4 – forward fan support, 5 – rear fan support, A – LRD.

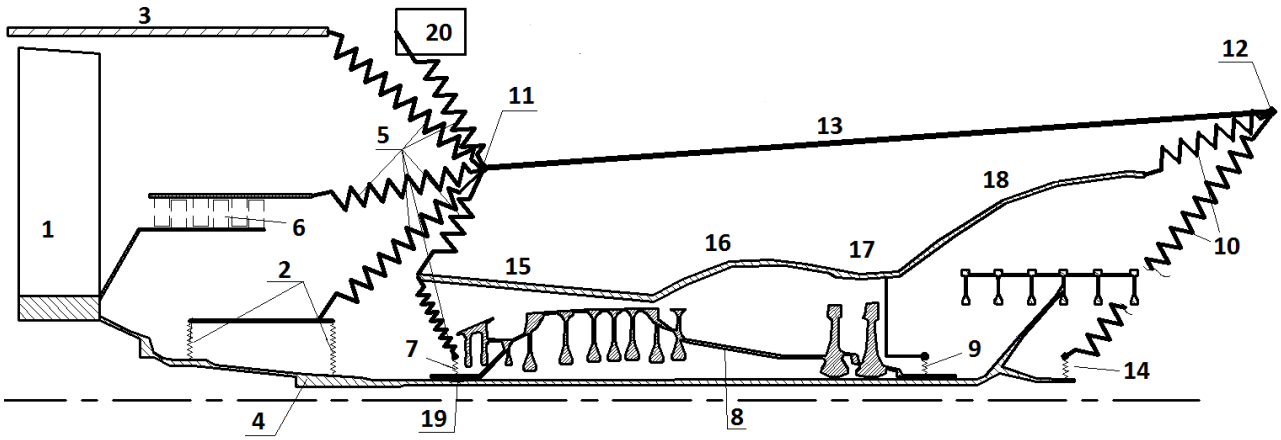

Figure 3. The simplified turbofan frame circuit.
1 – fan, 2 – fan supports, 3 – fan casing, 4 – LP shaft, 5 – intermediate casing, 6 – booster, 7 – HPC support flexible element and damper, 8 – HP rotor, 9 – HPT support flexible element and damper, 10 – LPT support, 11 – forward mount, 12 – backward mount, 13 – pylon, 14 – LPT support flexible element and damper, 15 – HPC casing, 16 – combustor casing, 17 – HPT casing, 18 – LPT casing, 19 – fan shaft interaction place, 20 – thrust reversal, aggregations.

parameters influence on engine dynamic behavior after FBO event.

The model proposed in the current research is relatively simple because it takes into account only considerable properties of engine. The simplified circuit of the turbofan engine is presented at fig 3.

Assumptions:

- unbalanced force is applied instantly in the initial modeling interval time moment
- no plastic deformations
- pylon is constrained in places of its junctions with airplane wing (airplane flexibilities aren't taken into account)
- LP rotor radial displacements are limited by means of low pressure compressor (LPC) blades and HP rotor in places with small clearance between shafts
- possible squeezing of HPC, HPT and LPT support dampers and appropriate stiffness change are taken into account
- friction between rotor and stator is taken into account only in rotors deceleration law and is eliminated from dynamic model
- LRD is breaks down at the FBO event moment

The most of engine frame units are modeled in the research using beam finite elements. These units are: LP and HP shafts, fan casing, booster casing, pylon, HPC, combustor, HPT and LPT casings. Some elements, such as fan supports, flexible elements of HPC, HPT and LPT supports are modeled as a simple springs. Thrust reversal and aggregations are taken into account as mass elements with supply of full 6x6 mass matrixes. Also such mass elements are used to correct whole engine model mass properties to match source data.

The complex 3D casings (intermediate casing and LPT support) can't be modeled as beams or as springs. These casings have a lot of flanges and any load applied to one flange influences on displacements and forces at all others. Full 3D FE models of casings aren't used in the transient process analysis because of considerable demands for computational time. Therefore method of Guyan reduction [3] is used here. This method allows calculating reduced stiffness and mass matrixes of casings based on full 3D FE models. All stiffness and inertial casings properties are condensed to degrees of freedom of condensation nodes. These nodes are situated either on the engine axis on corresponding flanges planes or at the engine mounts. The reduced matrixes are calculated once based on Guyan method derivations and then are included in full engine dynamic FE model to be used in transient nonlinear analysis at each time step. Thereby this method supplies account of stiffness and mass casing properties without significant computational time wastes.

Thereby 3D casings reduced stiffness and mass matrixes are assembled with corresponding beams matrixes, spring and mass elements into resulting whole engine stiffness and mass matrixes respectively. Dynamic problem is solved iteratively at each time step with account of linear elastic, inertial, damping, gyroscopic and nonlinear contact forces.

3 Contact interactions

Special NLRGAP elements (fig 4) are used for modeling contact interactions:

- between rotor and stator in HPC
- between shafts near HPC and HPT supports
- in HPC, HPT and LPT damper supports to take into account possible damper squeezing and support stiffness change

This element type has inner (A) and outer (B) nodes corresponding to rotor and stator (or LP and HP rotor in the case of shafts interaction) respectively and situated in coinciding geometrical points of the engine model. The radial clearance is specified. If relative nodes displacement overcomes radial clearance, the NLRGAP element produces in general nonlinear elastic force depending on the radial penetration.

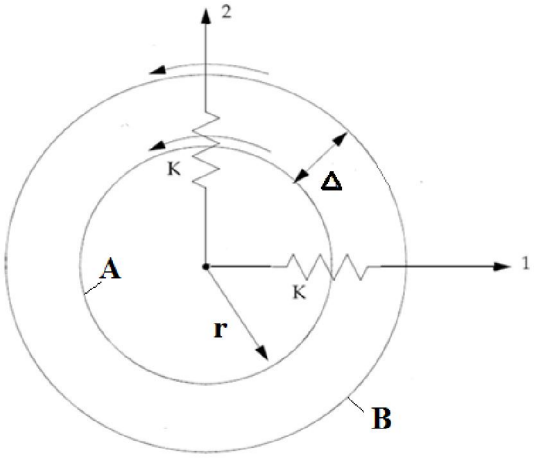

Figure 4. NLRGAP element
r – shaft radius, A – inner node, B – outer node, k – contact stiffness, Δ – clearance between rotor and stator.

In the case of rotor-stator interaction by means of blades the nonlinear elastic contact force law is dependent on corresponding stage blade properties and is computed using 3D FE nonlinear static analysis. The example of nonlinear single blade elastic characteristic is presented at fig 5. All nonzero contact forces of the current stage blades are summarized through the circle resulting in whole stage nonlinear contact characteristic.

In the case of shafts interaction or damper squeezing the elastic contact force law is assumed to be linear. Contact region doesn't contain any flexible bodies and the contact flexibility tends to zero. The value of the appropriate contact stiffness ought to be chosen based on considerations of contact modeling accuracy and numerical convergence. Therefore the chosen contact stiffness is not much higher than a typical engine frame element stiffness and usually is equal $1{,}0*10^7$ N/mm.

Further modeling results of the turbofan engine dynamics after FBO event are adduced.

4 Analysis of LRD introduction influence on turbofan strength circuit

Forward mount force time dependences after FBO event at maximum operating rotating frequency are presented at fig 6. There cases of LRD existence and absence in the 1st fan support are considered. Here and further forces are measured in fractions of the unbalanced fan

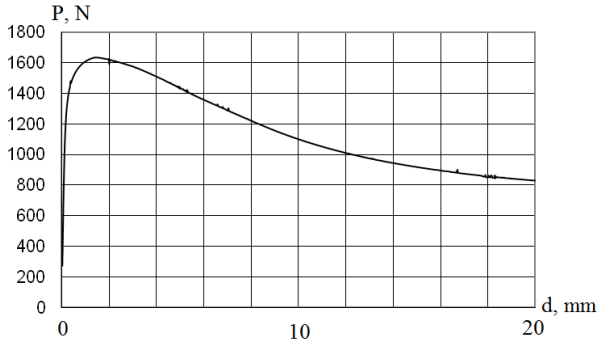

Figure 5. The example of single blade elastic characteristic.
P – elastic contact force, d – penetration.

blade centrifugal force at the maximum operation speed. There are two stages in the process: transient – after instant applying of the unbalanced fan blade centrifugal force, and stationary. We can see from the figure that LRD introduction reduces maximum forward mount force in ~4 times, and maximum force at steady vibration mode on maximum operating rotation frequency – in ~2,5 times. Other turbofan frame elements loads are changed similar way with LRD introduction.

Let's consider LRD introduction influence on the maximum forward mount force at steady vibration mode. The full rotation frequency range (from autorotation angular speed to maximum operating speed) is analyzed. The corresponding force dependence on the rotation frequency is presented at the fig 7. Here and further rotation frequency is measured in fractions of the maximum operating rotating frequency.

System changes its characteristic from red to green one after LRD actuation. We can see resonance maximums on both characteristics (without LRD – on frequency 0,8, with LRD – 0,45). It should be noted that these maximums values may considerably differ from critical rotor speed values because of contact interactions.

The engine is operating on the maximum rotating frequency (matches 1,0 on the absciss axis at fig 7) when FBO event happens. After fuel turning off turbofan rotors decelerate, passing through resonances to autorotation region. Maximum forces are achieved not after FBO but with resonances passing.

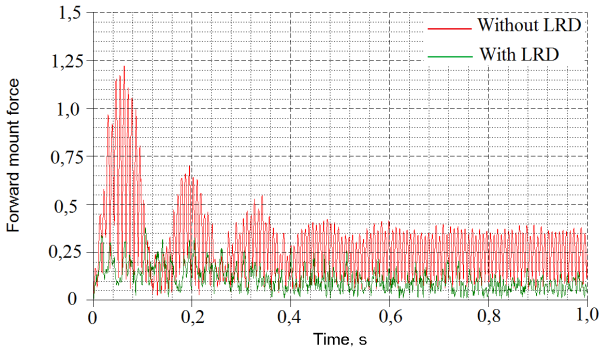

Figure 6. Forward mount force time dependence after FBO event. Rotors run at maximum operating rotating frequency.

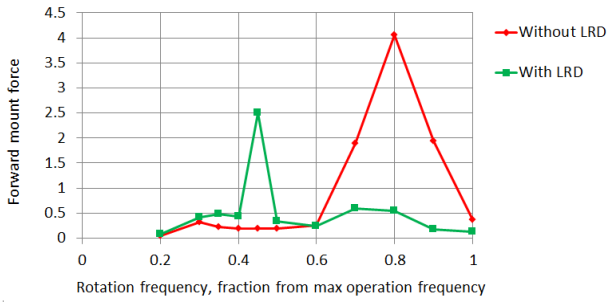

Figure 7. The rotation frequency dependence of maximum forward mount force on steady vibration mode after FBO event.

Basing on publication [1] data let's take rotors deceleration law as shown at fig 8. We assume that fuel feed is turned off in 1 s after FBO event. Thereby we can stress three stages of the process:

1. Operating at the maximum rotating frequency during 1st second after FBO event.
2. Rotors deceleration during 2nd second till the autorotation frequency (is equal to 0,2 from maximum operating rotating frequency).
3. Autorotation mode operating till landing.

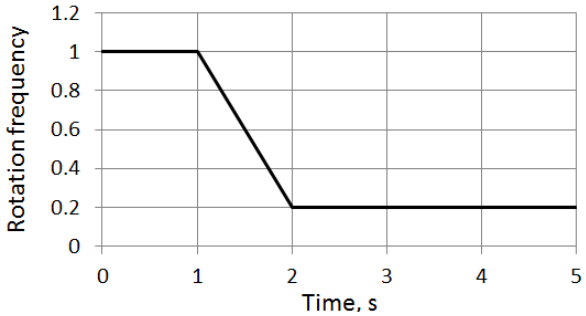

Figure 8. Rotors operating frequency time dependence after FBO event.

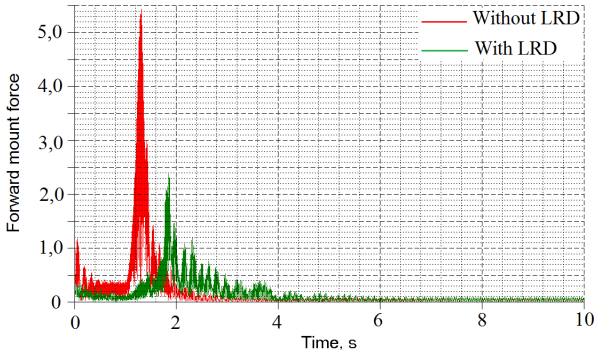

Figure 9. Turbofan engine forward mount force time dependences after FBO event.

Turbofan engine forward mount force time dependences according accepted rotors deceleration law after FBO event are presented at fig 9. We can see that LRD introduction doesn't significantly change steady vibration mode maximum force at autorotation frequency and reduces maximum loads achieved on the resonances passing in ~2,4 times.

Thereby it has been shown that LRD introduction in 1st fan support considerably reduces maximum frame loads after FBO event. The case of LRD absence in the 1st fan support is not considered below.

5 The investigation of some turbofan engine parameters influence on frame loads after FBO event in the case of LRD existence in the 1st fan support

After conclusion about LRD introduction effectiveness let's answer two questions:

- how can we provide maximum LRD introduction effectiveness?
- how can we provide shafts interactions absence on autorotation steady vibration mode?

The fan 2nd support stiffness dependence of the maximum forward mount force after FBO event is presented at fig 10. The nominal stiffness is assumed to be equal to unity. Computations shown that in the case of LRD absence in the 1st fan support the maximum force doesn't significantly depend on 2nd support stiffness.

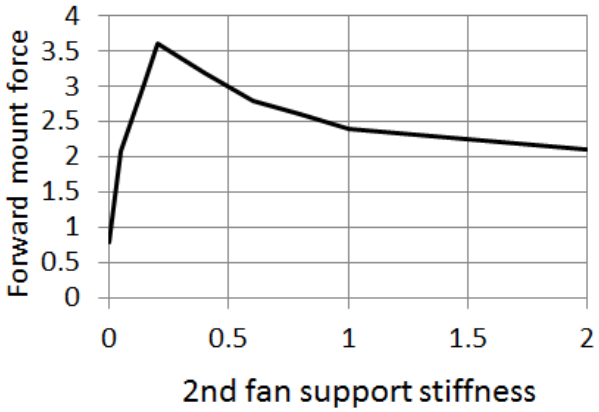

Figure 10. Maximum forward mount force dependence on the fan 2nd support stiffness, in the nominal stiffness fractions. There is the LRD in the 1st fan support.

We can see from the figure that we can achieve further turbofan engine frame loads reducing by means of either 2nd support stiffness increase or significant decrease. But any 2nd support stiffness change results in engine resonance adjustment disturbance. Therefore it may be reasonable to consider the additional LRD introduction in the 2nd fan support. We can't allow full 2nd fan support disconnection because it results in reducing of number of regular LP rotor supports to 1 and considerable loads would be past either through shaft interaction places or through LPC blades. Thereby it may be reasonable to introduce to the 2nd support a LRD supplying specified stiffness reducing after FBO event. Examples of two LRD introduced see [4].

Now let's consider shaft interaction contact force time dependences near HPC and HPT supports (see fig 11). We can see that shaft interaction doesn't stop on autorotation mode that may results in their rupture. Computations showed that full avoidance of shaft interaction after FBO event is not possible. Let's investigate conditions for avoidance of continuous shaft interaction on autorotation mode. Contact forces time dependences are presented at fig 12 for the case of doubled radial clearances. We can see that there is no shaft interaction on the autorotation steady vibration mode (see interval [7; 10]) in this case.

Thereby it's reasonable for shaft interaction avoidance on the autorotation mode to increase shaft clearance near HPC and HPT supports.

The dependence of maximum forward mount force after FBO event on the 2nd fan support stiffness for the case of doubled clearances is presented at fig 13. We can see that there is a region of relatively small forward mount forces in the case of low stiffness values.

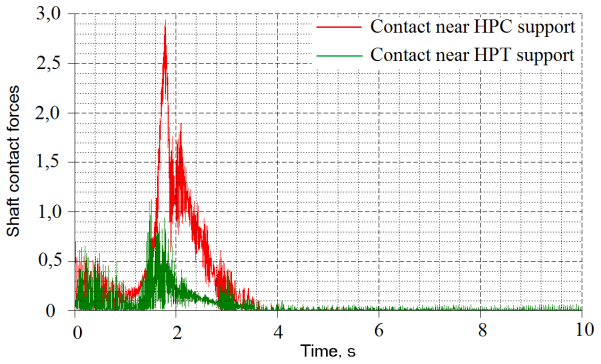

Figure 11. Shaft interaction contact force time dependences after FBO event. There is the LRD in the 1st support.

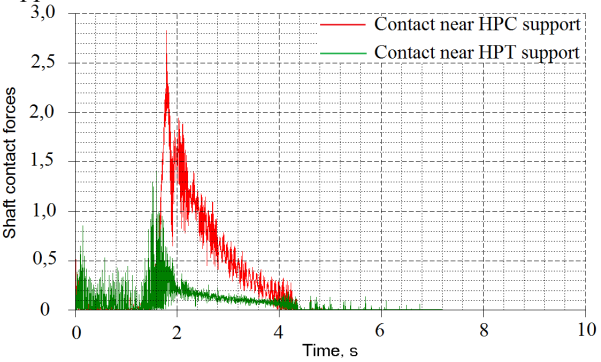

Figure 12. Shaft interaction contact force time dependences after FBO event. There is the LRD in the 1st support, radial shaft clearances are doubled.

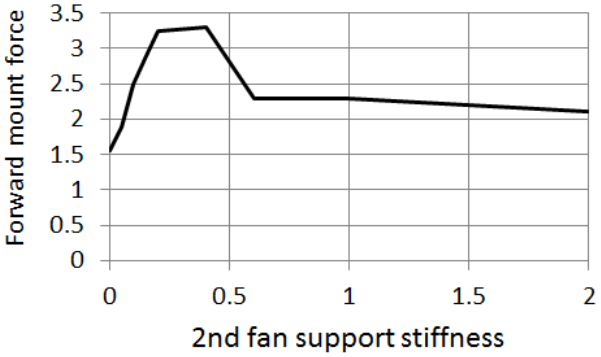

Figure 13. Forward mount maximum force dependence on the 2nd fan support stiffness, in nominal stiffness fractions. There is the LRD in the 1st support, radial shaft clearances are doubled.

6 Conclusions

The model for engine frame dynamic displacements and forces computation in the case of FBO event is adduced in the research work. It has been shown that special breakable elements introduction to 1st fan support results in significant engine elements maximum loads reducing. Additional analysis shown:

- it's reasonable to increase shaft clearances for shaft interaction avoidance on the autorotation mode
- additional LRD can result into supplementary engine frame loads reducing

References

[1] Carney K.S., Lawrence C., Carney D.V. Aircraft Engine Blade-Out Dynamics. *7th International LS-DYNA Users Conference,* Salzburg, Vol. 1, pp.17-26, 2009.

[2] Husband J.B. *Developing an Efficient FEM Structural Simulation of a Fan Blade Off Test in a Turbofan Jet Engine*. 1st edition, University of Saskatchevan, 2001.

[3] Bathe K.-J. *Finite Element Procedures*. 1st edition, New Jersey: Prentice Hall, 1996.

[4] Ivanov I.I. On the choice of parameters of device to reduce load on components of turbojet engine pressure vessels after fan blade breakage. *Proceedings of higher educational institutions. Machine building*, Vol. 10, No. 1, pp. 3-11, 2001. (*in Russian)*.

Copyright Statement